Excitons and polaritons in monomolecular layers

Michael R. Philpott
IBM Research Laboratory, San Jose, California 95193

Peter G. Sherman
Institute of Theoretical Science and Department of Chemistry, University of Oregon, Eugene, Oregon 97403

(Received 11 June 1975)

A theory of the coupling of photons to the exciton states of a monomolecular layer is presented. It is shown that the collective excitations (polaritons) of the layer are of mixed exciton-photon character. For transitions polarized perpendicular to the exciton wave vector there are two polariton branches, one is superradiant with radiative lifetimes $(\lambda/a)^2 \simeq 10^4$ times *shorter* than for the free molecule, and the other does not radiate at all. This subradiant branch is defined for all frequencies ω below the molecular transition frequency ω_0 and for $\omega \ll \omega_0$ corresponds to an electromagnetic wave trapped on the monolayer. The properties of polaritons on monolayers near the plane interface of two media are considered and the polariton dispersion relation examined for some special cases.

I. INTRODUCTION

A planar two-dimensional sheet of molecules has optical properties that resemble neither those of the constituent molecules nor those of a bulk crystal obtained by stacking a large number of layers one on top of the other. Unique properties characteristic of very thin layers arise because all molecules are surface molecules, experiencing lateral interactions but no interactions in directions perpendicular to the layer. The reduction in dimensions causes the appearance of several new phenomena, in particular the trapping of electromagnetic waves about the surface and the occurrence of excited states with large radiative widths (superradiant states).

Monomolecular layers can be assembled in a number of ways depending on the nature of the molecule and the substrate upon which it is deposited. Fatty acid layers can be formed and handled using dipping-tank techniques.[1] Monolayers of numerous smaller molecules can be deposited routinely on ultraclean metal surfaces.[2] Expitaxial growth of one material on another allows the formation of crystalline layers of microscopic thinness. Monolayers also occur naturally as the subunits in biological membranes and lipid bilayers.[3]

In this paper we consider the optical properties of a monomolecular layer first in isolation and then near the surface of an optically denser medium. The molecules are assumed to be arrayed as in a two-dimensional crystal with identical orientations and uniform spacings. This model is admittedly something of an abstraction, for many of the monolayers referred to in the preceding paragraph probably have short-range but no long-range order. Exceptions are certain planar aromatic hydrocarbons on inert Pt (111) surfaces, where low-energy-electron-diffraction (LEED) patterns show that the monolayer is a two-dimensional crystal.[2] In any case the contribution to the local field at any site from long-range interactions between molecules is much more sensitive to relative orientation than to the separation, so that for molecules with roughly equal in-plane polarizability components the model should hold. In some monolayers the anisotropy of molecular interactions may serve to lock in long-range order, as, for example, in Kuhn's brickwork model of mixed fatty acid monolayers, so for these systems the model is also realistic.

In the monolayer systems referred to above it is implicit that the molecules of the monolayer and supporting substrate are chemically distinct. This is obviously a sufficient but not a necessary difference, for if the molecules are physically differentiable, then a monolayer with distinct properties will exist. At every crystal surface the molecules of the first plane differ from deeper lying molecules by the absence of van der Waals and electron exchange interactions from one side. In certain experiments the surface plane may behave as a monolayer provided the interactions between the surface and deeper lying planes serve to isolate the phenomenon at the surface. There is growing experimental evidence that this effect occurs for the (001) planes of crystalline linear polyacenes (anthracene and tetracene) and the surface plane behaves as a completely ordered monolayer of macroscopic area.[4–6]

Microscopic theories of the optical properties of monolayers have concentrated mainly on providing a basis for understanding ellipsometric measurements.[7–10] Agranovich and Dubovskii[11(a)] have derived a polariton relation for a two-dimensional crystal in which the dipole transitions are perpendicular to the plane. They found that for real wave vectors $\vec{\kappa}$ the polariton had two branches, one

heavily damped and the other undamped. Some aspects of coherence during the radiative decay of excitons in monolayers and thin multilayers have been described by Lee *et al.*[11(b)] The theory presented here is a sequel to an earlier paper,[12] and considers all three possible orientations of the transition dipole, the nature of polariton and exciton bands in two dimensions, resonances in the scattering amplitudes for incident light beams, and the effect on the polariton branches of a substrate surface in close proximity to the monolayer. For the isolated monolayer two types of radiative modes are examined: First, modes with complex frequency and real wave vector $\vec{\kappa}$, and second, the more useful constant-angle virtual modes (CAVM) for which the complex frequency and complex wave vector have the same phase. For the nonradiative region, $\kappa > \omega/c$ where the frequencies are real the two types of modes are identical.

This paper is organized as follows: In Sec. II we present some general remarks on the nature of the problem and the types of solution expected. In Sec. III the optical properties and the polariton dispersion relation for an isolated monolayer are derived. In Sec. IV the theory for a layer a distance h from the surface of a half-space of an optically denser medium is outlined. Finally in Sec. V a brief discussion and some comments concerning polaritons in the surface planes of aromatic hydrocarbons are presented.

II. FORMULATION OF THE PROBLEM

We use the classical oscillator theory of excitons and polaritons in molecular aggregates[13] thereby neglecting all nonlinear processes. The response of a molecule at site $\vec{r}_s$ to an exciting field with time dependence $e^{-i\omega t}$ is governed by a set of oscillating dipoles $\vec{d}_{su}e^{-i\omega t}$, where u denotes a transition from the ground level to an excited state u. After cancellation of the factor $e^{-i\omega t}$ the equations of motion for an aggregate of molecules in vacuum become

$$\sum_{s'} [\vec{\vec{1}}\delta_{ss'} + 4\pi\vec{\vec{\alpha}}_s(\omega)\cdot\vec{\vec{\Phi}}_{ss'}(\omega)]\cdot\vec{P}_{s'} = \vec{\vec{\alpha}}_s(\omega)\circ\vec{E}'(\vec{r}_s)\,, \tag{2.1}$$

where $\vec{\vec{\alpha}}_s(\omega)$ is the polarizability, $\vec{\vec{\Phi}}_{ss'}(\omega)$ is a dimensionless retarded dipole-dipole interaction defined by

$$(4\pi/v_c)\vec{\vec{\Phi}}_{ss'}(\omega) = -[\vec{\nabla}\vec{\nabla} + (\omega/c)^2\vec{\vec{1}}]R^{-1}e^{i\omega R/c}\,, \tag{2.2}$$

with

$$R = |\vec{r}_s - \vec{r}_{s'}|\,, \tag{2.3}$$

v_c is a unit-cell volume, which can be chosen in any convenient way, and $\vec{P}_s$ is a vector defined by

$$\vec{P}_s = v_c^{-1}\sum_u \vec{d}_{su}\,. \tag{2.4}$$

For point molecules in a medium of dielectric constant ϵ we must replace ω/c by $\epsilon^{1/2}\omega/c$ and R^{-1} by $(\epsilon R)^{-1}$ in Eq. (2.2).

In Eq. (2.1) the structure of the driving field depends on whether or not there is an incident light beam and whether or not there is a substrate surface near the monolayer. In the absence of a surface and incident field the solutions of the equations of motion represent the normal modes of the monolayer. If the normal-mode frequency satisfying

$$\det|\vec{\vec{1}}\delta_{ss'} + 4\pi\vec{\vec{\alpha}}_s(\omega)\cdot\vec{\vec{\Phi}}_{ss'}(\omega)| = 0 \tag{2.5}$$

is real, the state is stationary and not subject to radiative decay. On the other hand, modes with complex frequencies represent virtual states of the system that have finite lifetimes owing to radiactive decay. We shall show that an isolated monolayer has both sorts of mode and that some are definitely polariton in character owing to strong coupling of exciton and photon states.

To obtain the Coulombic exciton states of the monolayer one lets $c\to\infty$ in Eq. (2.5). The exciton levels have frequencies that satisfy

$$\det|\vec{\vec{1}}\delta_{ss'} + 4\pi\vec{\vec{\alpha}}_s(\omega)\cdot\vec{\vec{V}}_{ss'}| = 0\,, \tag{2.6}$$

where $\vec{\vec{V}}_{ss'}$ is the static point dipole-dipole interaction defined by

$$(4\pi/v_c)\vec{\vec{V}}_{ss'} = R^{-3}(\vec{\vec{1}} - 3\hat{R}\hat{R})\,,$$

with $\hat{R} = (\vec{r}_s - \vec{r}_{s'})/R$.

III. ISOLATED MONOLAYER

In this section we begin by examining the types of exciton band and polariton states of a two-dimensional crystal of identical molecules using the dipole approximation for intermolecular interactions. For convenience it is assumed that the unit cell is a square with edge length a.

The sites of the lattice are

$$\vec{r}_{nm} = na\hat{x} + ma\hat{y}\,, \tag{3.1}$$

where $\hat{x}$ and $\hat{y}$ are unit vectors parallel to the edges of the primitive unit cell and n and m are integers. Periodic boundary conditions are assumed. The plane of the lattice is defined by $z=0$, so that the unit vector $\hat{z}$ is perpendicular to the plane of the monolayer.

A. Coulombic exciton states of a monolayer

For molecules with only a single excited state and a nondegenerate ground state the polarizability is

$$4\pi\vec{\vec{\alpha}}(\omega) = [\omega_p^2 f_0/(\omega_0^2 - \omega^2)]\hat{d}\hat{d}\,, \tag{3.2}$$

where ω_0 is the excitation frequency, $\hat{d}$ is a unit

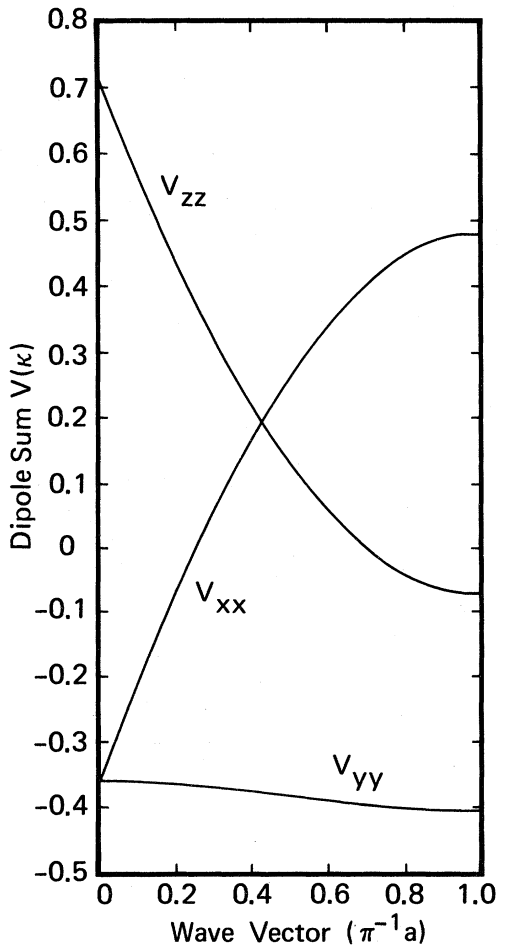

FIG. 1. κ dependence of the two-dimensional dipole sums V_{xx}, V_{yy}, and V_{zz} of the square lattice for $\vec{\kappa}$ parallel to the x axis.

vector parallel to the transition dipole, f_0 is the oscillator strength

$$f_0 = 2m_e\omega_0\mu_0^2/\hbar e^2 , \tag{3.3}$$

μ_0 is the transition dipole moment, and ω_p is the "plasma" frequency defined by

$$\omega_p^2 = 4\pi e^2/m_e v_c . \tag{3.4}$$

The Coulombic exciton with wave vector $\vec{\kappa}$ belonging to a two-dimensional Brillouin zone has a frequency [from Eqs. (2.6) and (3.2)] given by

$$\omega_{ex}^2(\vec{\kappa}) = \omega_0^2 + 2\omega_p^2 f_0 \hat{d}\cdot\vec{\vec{V}}(\vec{\kappa})\cdot\hat{d} , \tag{3.5}$$

where

$$\vec{\vec{V}}(\vec{\kappa}) = \sum_{s\neq s'} \vec{\vec{V}}_{ss'} e^{i\vec{\kappa}\cdot(\vec{r}_s - \vec{r}_{s'})} \tag{3.6}$$

is a phase-modulated dipole sum for the two-dimensional lattice.

Several methods are known for rapidly computing dipole sums in a planewise fashion.[14,15] To illustrate the dispersion of the two-dimensional exciton band we have calculated the diagonal components of $\vec{\vec{V}}(\vec{\kappa})$ for wave vectors $\vec{\kappa}$ parallel to the x axis and transition dipoles $\hat{d}$ oriented along $\hat{x}$, $\hat{y}$, and $\hat{z}$. The formulas of Benson and Mills[15] have been used in these calculations and the results are displayed in Fig. 1. Note that $V_{yy}(\vec{\kappa})$ has almost no dispersion because of cancellations among the long-range interactions that occur when $\hat{d}$ lies in the plane and is perpendicular to $\vec{\kappa}$. For the other two components the long-range interactions do not cancel and their complementarylike behavior is determined by the sum rule[14]

$$V_{xx}(\vec{\kappa}) + V_{yy}(\vec{\kappa}) + V_{zz}(\vec{\kappa}) = 0 . \tag{3.7}$$

The initial linear dependence on κ clearly visible in Fig. 1 for the x and z sums comes from the long-range contribution

$$\pm (v_c/4\pi)(2\pi/a^2)\kappa ,$$

with the upper and lower signs for V_{xx} and V_{zz}, respectively.

The results imply that s-polarized Coulombic excitons (E vector perpendicular to the plane of incidence) have little or no dispersion, whereas p-polarized Coulombic excitons (E-vector parallel to the plane of incidence) may exhibit strong dependence on the projection of the photon wave vector onto the plane of the monolayer.

B. Polariton states of a monolayer

To simplify the problem of coupling excitons to photons a polarizability tensor like that of Sec. III A is used. However, to include the radiation field in a consistent way, Eq. (3.2) must be amended to include a term describing the radiative damping of the transition in the free molecule. Therefore we set

$$4\pi\vec{\vec{\alpha}}(\omega) = \frac{\omega_p^2 f_0}{\omega_0^2 - \omega^2 - i\omega^3\gamma_0}\hat{d}\hat{d} , \tag{3.8}$$

where[16,17]

$$\gamma_0 = (2e^2/3m_e c^3) f_0 . \tag{3.9}$$

Nonradiative damping terms may also be included in the denominator of $\vec{\vec{\alpha}}(\omega)$ if it is desired to simulate the effects of other relaxation processes.

After substitution of Eq. (3.8) into Eq. (2.1) we find for the polariton (coupled exciton-photon) states of wave vector $\vec{\kappa}$ the following dispersion equation:

$$\omega^2 = \omega_0^2 - i\omega^3\gamma_0 + 2\omega_p^2 f_0 \hat{d}\cdot\vec{\vec{\Phi}}(\vec{\kappa},\omega)\cdot\hat{d} , \tag{3.10}$$

where

$$\vec{\vec{\Phi}}(\vec{\kappa},\omega) = \sum_{s\neq s'} \vec{\vec{\Phi}}_{ss'}(\omega) e^{i\vec{\kappa}\cdot(\vec{r}_s - \vec{r}_{s'})} \tag{3.11}$$

is a phase-modulated sum of retarded dipole interactions for the two-dimensional lattice.

We consider the cases where the transition dipole direction $\hat{d}$ points along $\hat{x}$, $\hat{y}$, or $\hat{z}$, while $\vec{\kappa} = \kappa\hat{x}$ has a fixed direction. The problem is now to calculate the diagonal components of the tensor $\vec{\Phi}(\vec{\kappa}, \omega)$. To find these components a trick is used. First we write down the Hertz vector of the array of dipoles as a sum of Hertz vectors for each dipole. The Hertz vectors are then represented in the form of a double integral,[18] and the lattice sum converted to the equivalent reciprocal sum. Differentiation gives the electric field at any point not coincident with the lattice points. Then the limit $\vec{r} \to \vec{r}_s$ (sth lattice site) is taken and the self-fields of site s subtracted. In the resulting expression it is possible to identify the long-range radiative, long-range static, and short-range static dipole interactions.

1. *Dipoles perpendicular to the plane ($\hat{d} = \hat{z}$)*

For dipoles perpendicular to the plane of the monolayer $\hat{d} = \hat{z}$ and $\hat{d} \cdot \vec{\kappa} = 0$. In a medium of dielectric constant ϵ, the z component of the Hertz vector for an array of dipoles

$$\vec{d}_s(t) = d\, e^{i(\vec{\kappa}\cdot\vec{r}_s - \omega t)}\hat{z} \tag{3.12}$$

is

$$\Pi_z(\vec{r}, t) = \frac{d}{\epsilon}\sum_s R_s^{-1} e^{i(\vec{\kappa}\cdot\vec{r}_s + kR_s - \omega t)} , \tag{3.13}$$

where $k = \epsilon^{1/2}\omega/c$. The x and y components are zero. Next we use the double integral representation[18]

$$\frac{e^{ikR}}{R} = \frac{1}{2\pi}\int\int_{-\infty}^{\infty} \frac{e^{i(\xi x + \eta y)} e^{-\gamma|z|}}{\gamma} , \tag{3.14}$$

where

$$\gamma = (\lambda^2 - k^2)^{1/2} , \tag{3.15}$$

$$\lambda^2 = \xi^2 + \eta^2 , \tag{3.16}$$

$$\lim_{\lambda \to 0} \gamma = -ik , \tag{3.17}$$

to transform the lattice sum to one over the reciprocal lattice, giving

$$\Pi_z(\vec{r}) = \frac{2\pi d}{\epsilon a^2}\sum_{\vec{G}} \gamma^{-1} e^{i\vec{g}\cdot\vec{r} - \gamma|z|} , \tag{3.18}$$

with

$$\vec{g} = \vec{\kappa} + \vec{G} , \tag{3.19}$$

$$\gamma = (g^2 - k^2)^{1/2} . \tag{3.20}$$

Note that γ depends explicitly on the reciprocal vectors $\vec{G}$. The z component of the electric field at $\vec{r}$ is

$$E_z(\vec{r}) = \left(\frac{\partial^2}{\partial z^2} + k^2\right)\Pi_z(\vec{r}) \tag{3.21}$$

$$= \frac{2\pi d}{\epsilon a^2}\sum_{\vec{G}} \frac{g^2}{\gamma} e^{i\vec{g}\cdot\vec{r} - \gamma|z|} , \tag{3.22}$$

and the polariton dispersion, Eq. (3.10), can be written

$$\omega^2 = \omega_0^2 - i\omega^3\gamma_0 - (e^2 f_0/m_e d)E_z'(0) , \tag{3.23}$$

where $E_z'(0)$ is the exciting field at site $\vec{r}_s = 0$ obtained from Eq. (3.22) by taking the limit $\vec{r} \to 0$ after subtracting the self-field of the site $s = 0$. The exciting field

$$d^{-1}E_z'(0) = -v_z(\kappa) - i\tfrac{2}{3}k^3 + (2\pi\kappa^2/a^2\epsilon)(\kappa^2 - k^2)^{-1/2} \tag{3.24}$$

consists of a real short-range dipole field v_z, a radiative term from the imaginary part of the self-field of site $s = 0$, and a long-range dipole field from the $\vec{G} = 0$ term of Eq. (3.22) that is pure imaginary (radiative) for $k > \kappa$.[19] The field $v_z(\kappa)$ has no $\vec{G} = 0$ term in an expansion over the reciprocal lattice and is independent of $a\kappa$ to order $(a\kappa)^2$ for wave vectors satisfying $a\kappa \ll 1$. This behavior is in sharp contrast to that of $V_{xx}(\kappa)$ and $V_{zz}(\kappa)$, which depend linearly on $a\kappa$ (see Fig. 1) for $a\kappa \ll 1$. Since $v_z(\kappa)$ is basically the Coulomb sum with the long-range term subtracted, we have $v_z(\kappa) = (4\pi/v_c)V_{zz}(0)$.

If we define an exciton frequency $\omega_z(\kappa)$ in analogy with Eq. (3.5) by

$$\omega_z^2(\kappa) = \omega_0^2 + (e^2 f_0/m_e)v_z(\kappa) , \tag{3.25}$$

then the polariton dispersion equation is

$$F_z(\omega, \kappa) = 0 , \tag{3.26a}$$

where

$$F_z(\omega, \kappa) = \omega_z^2(\kappa) - \omega^2 - \frac{2\pi e^2 f_0}{\epsilon m_e a^2}\frac{\kappa^2}{(\kappa^2 - k^2)^{1/2}} . \tag{3.26b}$$

Since only the short-range part of the interaction is included in $\omega_z(\kappa)$, the exciton is analogous to the mechanical exciton of Agranovitch and Ginzburg.[20]

Note that if $k > \kappa$, then we replace $(\kappa^2 - k^2)^{1/2}$ by $-i(k^2 - \kappa^2)^{1/2}$ to retain consistency with requirement (3.17). We also require $\mathrm{Re}\gamma > 0$ in order that the electric fields calculated from the Hertz vector (3.18) are to be bounded. This means that the physical solutions of Eq. (3.26a) must be such that $\mathrm{Re}(\kappa^2 - k^2)^{1/2} > 0$. Furthermore, since we are interested in the radiant decay of prepared states, for which $\mathrm{Im}\omega < 0$, and the properties of subradiant states, for which $\mathrm{Im}\omega = 0$, the solutions of Eq. (3.26a) of physical interest lie either in the lower half of the complex ω plane or on the real ω axis. The use of the double-integral representation (3.14) for $R^{-1}e^{ikR}$ implies that the function $F_z(\omega, \kappa)$ [Eq. (3.26b)] is defined only for $k = \beta + i\sigma$ ($\sigma > 0$), so that if solutions of Eq. (3.26a) are desired for $k = \beta - i\sigma$ ($\sigma > 0$), the function must first be defined there by analytic continuation.

Modes with real κ and complex ω are considered separately from those with complex κ and complex ω. The former type we refer to as "real-κ" modes and the latter type as constant-angle virtual modes (CAVM) for reasons given later. In the nonradiative region where $\kappa > \omega/c$ the real-κ and constant-angle modes are identical, so it is logical to first discuss the properties of this nonradiative or subradiant branch, as we prefer to call it.

It is a straightforward matter to show by considering the form of Eq. (3.26b) for $\kappa \simeq 0$ and $\omega \simeq 0$ that there exists a solution of Eq. (3.26a) with linear dependence on κ. The full branch has been found by squaring Eq. (3.26a) and solving for the root of the polynomial of the third degree in ω^2 that is real and satisfies the original unsquared equation. This branch lies to the right of the light line $\omega = c\kappa$ in the nonradiative region. It is shown in Fig. 2 near the point where it turns away from the light line and begins to follow the exciton line $\omega = \omega_z(\kappa)$. The parameters used in these and all subsequent calculations described in this paper are $f_0 = 1.0$, $\omega_0 = 3.0 \times 10^4\ \mathrm{cm}^{-1}$, $\epsilon = 1.0$, $v_c = a^3 = 100\ \text{Å}^3$, $\omega_z(\kappa = 0) = 4.2 \times 10^4\ \mathrm{cm}^{-1}$, and $\omega_x(\kappa = 0) = \omega_y(\kappa = 0) = 2.4 \times 10^4\ \mathrm{cm}^{-1}$. In Fig. 2 reduced variables $\omega_r = \omega/\omega_z(0)$ and $\kappa_r = c\kappa/\omega_z(0)$ have been used so that the equation of the light line is simply $\omega_r = \kappa_r$. The value of the oscillator strength is not unreasonably high (many dye molecules are known with transitions of this intensity), and the intermolecular spacing $a = 4.64$ Å is a good compromise between the thickness of aromatic molecules ($\simeq 3.5$ Å) and the intermolecular spacings in their solids.

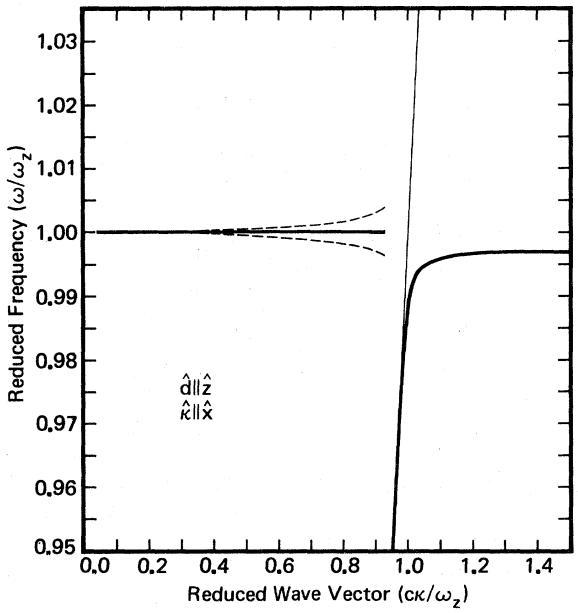

FIG. 2. Dispersion of the real-wave-vector polariton states of an infinite monolayer with dipoles perpendicular to the plane ($\hat{d} \| \hat{z}$, $\hat{k} \| \hat{x}$). There are two branches and the dashed lines show the width of the superradiant branch. The parameters for the calculation are $f_0 = 1.0$, $\omega_0 = 3.0 \times 10^4\ \mathrm{cm}^{-1}$, $v_c = a^3 = 100\ \text{Å}^3$, $\omega_z(0) = 4.2 \times 10^4\ \mathrm{cm}^{-1}$, $\omega_x(0) = \omega_y(0) = 2.4 \times 10^4\ \mathrm{cm}^{-1}$, and the reduced variables defined by $\omega_r = \omega/\omega_z(0)$ and $\kappa_r = c\kappa/\omega_z(0)$.

The states of the subradiant branch do not radiate because all photons with a component of momentum κ parallel to the monolayer lie higher in energy. From Eqs. (3.18) and (3.21) a subradiant state has an electric field that dies exponentially with perpendicular distance from the plane of the monolayer. For $\omega \ll \omega_z(0)$ the linear dependence on κ implies that the polariton is primarily photon-like and because the field is localized we describe the photon as being trapped about the plane of the monolayer. A more picturesque explanation is to attribute the trapping to the radiation patterns of the dipoles, which have lobes directed in the plane, so that there should be constructive interference in the direction κ mediated by the phase factor $e^{i\vec{\kappa}\cdot\vec{r}_s}$ of the dipoles. A long-range interaction between molecules results and a discrete state is split from the bottom of the one-dimensional continuum of photon states with wave vectors that project κ onto the monolayer.

Let us now consider if Eq. (3.26a) has any solutions on the left-hand side of the light line, which in quantum mechanics correspond to prepared states that decay by photon emission. For transition dipoles d perpendicular to the monolayer Agranovich and Dubovskii[11(a)] concluded that there was a radiative state with positive dispersion bending up away from the line $\omega = \omega_z(\kappa)$ as the light line was approached. This radiant branch should be obtainable from Eqs. (3.26a) and (3.26b): however, we have found that the analytic properties of $\gamma_\kappa = (\kappa^2 - k^2)^{1/2}$ do not permit physically acceptable solutions. For the dispersion equation (3.26a) to have a solution $k = \beta \pm i\sigma$ ($\sigma > 0$), we require $\mathrm{Re}\gamma_\kappa > 0$ for bounded fields at large distances z and $\mathrm{Im}\gamma_\kappa \gtrless 0$ in order for $\mathrm{Im}k \gtrless 0$. For a decaying state we require $\mathrm{Im}k < 0$. No choice of branch cuts was found for which γ_κ had the desired properties. For example, if the branch cut is chosen along the real-k axis from κ to ∞, then the sign of $\mathrm{Re}\gamma_\kappa$ changes on passing to the second sheet from $k = \beta + i\sigma$ ($\sigma > 0$) because the branch cut coincides with $\mathrm{Re}\gamma_\kappa = 0$. This does not necessarily mean that a real κ exciton prepared at time $t = 0$ will not exhibit exponential-like decay for some time regime. Rather it is a statement concerning the deformation of the contour of the integral determining the time-dependent amplitude of quantum theory. This contour cannot be deformed into separate contributions from an isolated pole and a hairpin traversing both Riemann sheets.

For real ω we have $\mathrm{Re}F_z(\omega, \kappa) = 0$ when $\omega = \omega_z$ so that an exponential-like decay of a prepared state is anticipated as long as $\mathrm{Im}F_z(\omega_z, \kappa)$ remains very

small. This is indeed the case for most of the interval $0 \le \kappa < \omega_z/c$ for $\mathrm{Im}F_z(\omega_z, \kappa) \to 0$ as $\kappa \to 0$ and is small for all κ except at values close to ω_z/c, where it diverges. Therefore we expect the decay of a real κ state to be characterized by an energy $\omega = \omega_z(0)$ and a width of magnitude $\mathrm{Im}F_z(\omega, \kappa)/(2\omega_z)$. This width is considerably larger than the radiative width of the transition in the isolated molecule for all except very small κ values because of the presence of a factor $(\omega_z a/c)^{-2} = (\lambda_z/a)^2 \simeq 10^4$. This can be seen more readily by writing Eq. (3.26b) as follows:

$$F_z(\omega, \kappa) = \omega_z^2(\kappa) - \omega^2 - i\frac{3\pi}{\epsilon}\frac{\omega^3\gamma_0}{(\omega a/c)^2} \times\left(\frac{c\kappa}{\omega}\right)^2\left[\left(\frac{c\kappa}{\omega}\right)^2 - \epsilon\right]^{-1/2} . \quad (3.27)$$

Here $\omega^3\gamma_0$, defined by Eq. (3.9), is the free-molecule damping and it is the presence of the factor $\omega^3\gamma_0(\omega a/c)^{-2} \simeq \omega^3\gamma_0 \times 10^4$ that justifies the label superradiant for this branch of the spectrum. In Fig. 2 the superradiant branch is shown by the horizontal solid line on the left of the light line flanked by dashed lines indicating how the width increases with κ. As the branch approaches the light line its width diverges, becoming comparable with ω_z so that it is not possible to assume it decays with an exponential-like behavior. Geometry determines the width at $\kappa = 0$, for then all dipoles are in phase and by analogy with the well-known results for a single oscillator[21] the field at great distances from the plane along the z axis is zero.

In a scattering experiment the real-κ radiative states with finite widths give rise to electromagnetic fields in which the direction of the wave vector differs from the direction of energy flow. In the usual optical experiment the scattered light is monitored at an angle θ from the surface normal and the dispersion curve is extracted by varying θ and using the relation $\kappa = (\omega/c)\sin\theta$ to determine the in-plane component of the wave vector. This requires that the direction of the wave vector and the energy flow be the same for the modes whose dispersion is being probed by such an experiment. The modes that satisfy this requirement are called constant-angle virtual modes (CAVM) by Kliewer and Fuchs.[22] For the CAVM, both frequency and wave vector are complex and when expressed in polar form the arguments of the complex frequency, the in-plane component of the wave vector, and the z component of the wave vector are identical.

We now proceed to determine the CAVM dispersion relation. Define

$$\omega_{\mathrm{CAVM}} = \omega_m e^{-i\phi} \quad (3.28a)$$

$$= \omega' - i\omega'' , \quad (3.28b)$$

$$\kappa_{\mathrm{CAVM}} = \kappa_m e^{-i\phi} \quad (3.29a)$$

$$= \kappa' - i\kappa'' , \quad (3.29b)$$

with ω_m and κ_m related by

$$\kappa_m = (\omega_m/c)\sin\theta . \quad (3.30)$$

Defining

$$\beta_{\mathrm{CAVM}} = -i\gamma = (\omega^2_{\mathrm{CAVM}}/c^2 - \kappa^2_{\mathrm{CAVM}})^{1/2} \quad (3.31)$$

leads to

$$\beta_{\mathrm{CAVM}} = (\omega_m/c)\cos\theta\, e^{-i\phi} . \quad (3.32)$$

Substitution of Eqs. (3.28)–(3.32) into the polariton dispersion (3.26), and equating the real and imaginary parts of each side gives the following simple results:

$$[\omega'(\theta)]^2 = \omega_z^2 - [\omega''(\theta)]^2 \quad (3.33)$$

and

$$\omega''(\theta) = \tfrac{1}{4}\omega_p^2 f_0 \sin^2\theta/\cos\theta . \quad (3.34)$$

Note that $\omega''(\theta) > 0$, consistent with the definition (3.28b) and the requirement of temporal damping. The variation of ω' and ω'' with θ is shown in Figs. 3 and 4, while the dispersion is displayed in Fig. 5. Note that the CAVM for this dipole orientation exhibits critical damping when θ is near grazing. The parameters used in these curves are the same as for the real-wave-vector modes. In Fig. 5 the radiative shift, defined as the difference between the exciton frequency and the central frequency of the mode, is about 35 cm^{-1}. When $\frac{1}{2}\pi - \theta = 5\times10^{-4}$

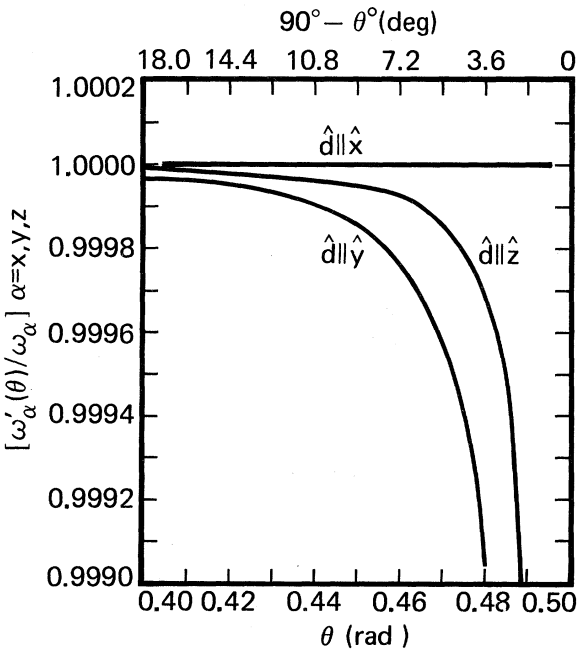

FIG. 3. Variation of the real part of the frequency of the constant angle mode ω'_{CAVM} with θ. The parameters are the same as in Fig. 2.

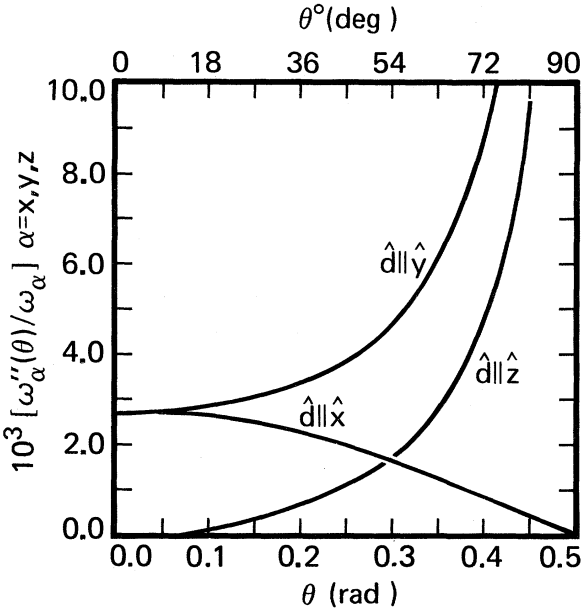

FIG. 4. Variation of the imaginary part of the frequency of the constant angle mode ω''_{CAVM} with θ. The parameters are the same as in Fig. 2.

or 0.09° up from grazing, we have $\omega''(\theta)=\omega_z(0)$, which defines the end point or the point of critical damping of the mode where the real and imaginary parts become equal.

2. Dipoles parallel to the wave vector $\vec{\kappa}$ ($\hat{d}\parallel\hat{x}$)

For transition dipoles parallel to the x axis we have $\hat{d}=\hat{x}$ and $\hat{d}\cdot\hat{\kappa}=1.0$. The Hertz vector for all the dipoles of the monolayer has only an x component. Omitting the time factor $e^{-i\omega t}$,

$$\Pi_x(\vec{r})=\frac{d}{\epsilon}\sum_s R_s^{-1}e^{i(\vec{\kappa}\cdot\vec{r}_s+kR_s)}, \tag{3.35}$$

and after transforming to a sum over reciprocal-lattice vectors

$$\Pi_x(\vec{r})=\frac{2\pi d}{\epsilon a^2}\sum_{\vec{G}}\gamma^{-1}e^{i\vec{g}\cdot\vec{r}-\gamma|z|}. \tag{3.36}$$

The x component of the electric field,

$$E_x(\vec{r})=\left(\frac{\partial^2}{\partial x^2}+k^2\right)\Pi_x(\vec{r}), \tag{3.37}$$

is needed to determine the polariton dispersion equation. The exciting field at site $\vec{r}_s=0$ is determined by the procedure described for the $\vec{d}\parallel\vec{z}$ case; we have for $\hat{d}=\hat{x}$ the result

$$d^{-1}E'_x(\vec{r}=0)=-v_x(\kappa)-i\tfrac{2}{3}k^3-(2\pi/\epsilon a^2)(\kappa^2-k^2)^{1/2}, \tag{3.38}$$

where $v_x(\kappa)$ is the short-range part of the static dipole field and the last term on the right-hand side of Eq. (3.38) comes from the $G=0$ part of the Hertz vector (3.36).

Next we introduce x-polarized excitons with frequency

$$\omega_x^2(\kappa)=\omega_0^2+(e^2f_0/m)v_x(\kappa). \tag{3.39}$$

The equation determining polariton frequency is given by $F_x(\omega,\kappa)=0$, where

$$F_x(\omega,\kappa)=\omega_x^2(\kappa)-\omega^2+(2\pi e^2f_0/\epsilon m_e a^2)(\kappa^2-k^2)^{1/2}. \tag{3.40}$$

An alternative equivalent form is

$$F_x(\omega,\kappa)=[\omega_x^2(\kappa)-\omega^2]+\frac{3\pi}{\epsilon}\frac{\omega^3\gamma_0}{(\omega a/c)^2}\left[\left(\frac{c\kappa}{\omega}\right)^2-\epsilon\right]^{1/2}, \tag{3.41}$$

where γ_0 is defined by Eq. (3.9) and $\omega^3\gamma_0$ is the damping term in the free-molecule polarizability [see Eq. (3.8)]. Squaring both sides gives a quadratic in ω^2 and the roots are therefore easy to obtain. The presence of $\gamma_\kappa=(\kappa^2-k^2)^{1/2}$ in Eq. (3.40) means, as in the previous $\vec{d}\parallel\vec{z}$ case, that the solution of the dispersion relation lying in the radiative region is not physically acceptable. However, the decay of a time-dependent amplitude of a prepared real-κ exciton state is expected to be exponential-like for the reasons explained earlier. There is only one branch with frequency $\Omega(\kappa)\simeq\omega_x(\kappa)$ for all κ. At $\kappa=0$ the polariton frequency is given by

$$\Omega^2(0)=\omega_x^2(0)-(i2\pi e^2f_0/\epsilon m_e a^2)k, \tag{3.42}$$

where we evaluate k at $\epsilon^{1/2}\omega_x(0)/c$. In Fig. 6 we have plotted the computed values of the real part

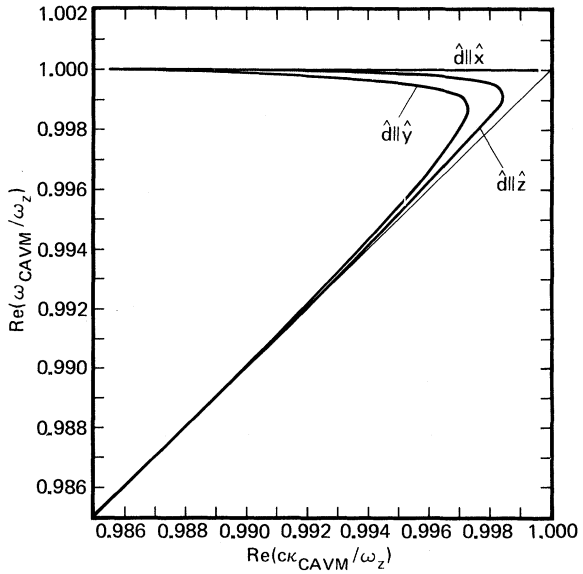

FIG. 5. Variation of the real part of ω_{CAVM} with the real part of κ_{CAVM}.

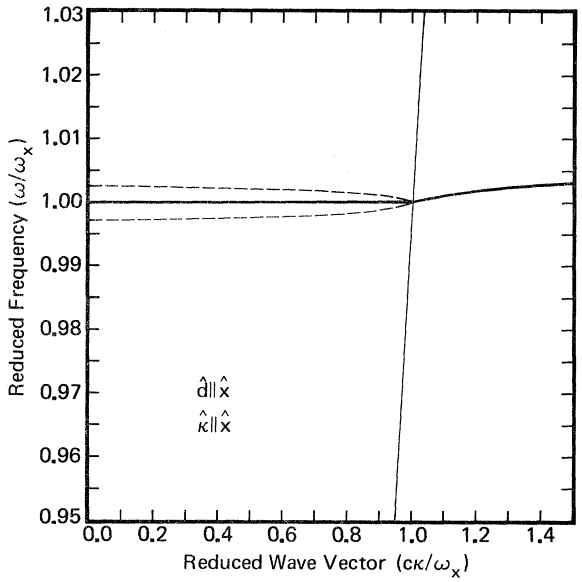

FIG. 6. κ dependence of the polariton frequency for a monolayer with $\hat{d} \parallel \hat{x}$. Wave vector $\vec{\kappa}$ is parallel to the x axis. There is one branch and the dotted lines show the width of the superradiant region. Same parameters are used as in Fig. 2.

of $\Omega(\kappa)$ and also the values of $\mathrm{Re}\Omega(\kappa) \pm \mathrm{Im}\Omega(\kappa)$. The width of the state at $\kappa = 0$ is considerably larger than the free-molecule width by a factor $(\lambda\!\!\!^{-}/a)^2 \simeq 10^4$ (in the optical region). As the light line is approached, the linewidth decreases and becomes zero, whereupon the state becomes a nonradiative exciton state with wave vector too large to allow photon emission into the vacuum with simultaneous conservation of energy and momentum. There are no trapped photon states for this orientation of the transition dipoles.

Unlike the case for transitions polarized either along x or y (see below) there is no separate subradiant branch for x-polarized transitions. Qualitatively this can be understood by looking at the radiation patterns of the dipoles which have lobes directed in directions perpendicular to $\vec{\kappa}$. Therefore, there are no components parallel to the plane of the monolayer and to $\vec{\kappa}$, which might be made to add constructively through the variations in the phase factor $e^{i\vec{\kappa}\cdot\vec{r}_s}$.

We can define CAVM frequencies and wave vectors as in Sec. III B1. In terms of θ the real and imaginary parts of the complex frequency of the virtual mode are

$$[\omega'(\theta)]^2 = [\omega_x(0)]^2 - [\omega''(\theta)]^2 \tag{3.43}$$

and

$$\omega''(\theta) = \tfrac{1}{4}\omega_p^2 f_0 a \cos\theta \,. \tag{3.44}$$

Note that the radiative width of the state

$$\gamma_{r,x}(\theta) = 2\omega''(\theta) \tag{3.45}$$

is well behaved for all values of θ and in particular does not become large as θ tends to $\frac{1}{2}\pi$. The dependence of ω' and ω'' on θ and on κ' is shown in Figs. 3–5. The radiative width has a maximum value for $\theta = 0$, where $\gamma_{r,x} \simeq 130\ \mathrm{cm}^{-1}$ for the parameters used in this calculation.

3. *Dipoles perpendicular to $\vec{z}$ and $\vec{\kappa}$ ($\hat{d} = \hat{y}$)*

When the transition dipoles lie in the plane of the monolayer and are perpendicular to the wave vector $\vec{\kappa}$ then $\hat{d}\cdot\hat{\kappa} = 0$ and $\hat{d}\cdot\hat{z} = 0$. The y component of the Hertz vector has the same form as the right-hand side of Eq. (3.35), and can be transformed into the same form as the right-hand side of Eq. (3.36) by using the representation for $R^{-1}e^{ikR}$ in Eq. (3.14).

The y component of the electric field at some arbitrary point outside the monolayer sites is given by

$$E_y(\vec{r}) = \left(\frac{\partial^2}{\partial y^2} + k^2\right)\Pi_y(\vec{r}) \,. \tag{3.46}$$

A direct calculation gives

$$E_y(\vec{r}) = \frac{2\pi d}{\epsilon a^2}\sum_{\vec{G}} (k^2 - g_y^2)\gamma^{-1} e^{i\vec{g}\cdot\vec{r} - \gamma|z|} \,, \tag{3.47}$$

where g_y is the y component of the vector $\vec{g} = \vec{\kappa} + \vec{G}$. Proceeding as for the last two orientations we find that the exciting electric field at the origin site is

$$d^{-1}E_y'(0) = -v_y(\kappa) - i\tfrac{2}{3}k^3 + (2\pi k^2/\epsilon a^2)(\kappa^2 - k^2)^{-1/2} \,. \tag{3.48}$$

In Eq. (3.48) $v_y(\kappa)$ is the short-range part of the static dipole sum. However, for this particular orientation there is no long-range part so that $v_y(\kappa)$ is also the full static dipole sum. The last term on the right-hand side of Eq. (3.48) comes from the $\vec{G} = 0$ term of the reciprocal-lattice sum in Eq. (3.47). Only the y-polarized excitation can be excited by s-polarized light, that is, light with an E field perpendicular to the plane of incidence (the xz plane). In a three-dimensional crystal s-polarized (transverse) excitons also do not have a long-range (macroscopic) dipole field.

The polariton dispersion relation is found, using Eq. (3.48), to be

$$F_y(\omega, \kappa) = 0 \,, \tag{3.49a}$$

where

$$F_y(\omega, \kappa) = \omega_y^2(\kappa) - \omega^2 - (2\pi e^2 f_0/\epsilon a^2 m_e)k^2(\kappa^2 - k^2)^{-1/2} \,. \tag{3.49b}$$

An alternative way of writing this relation is

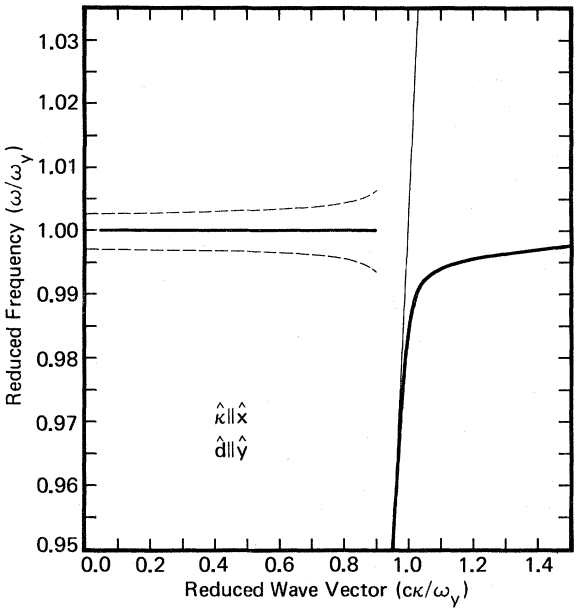

FIG. 7. κ dependence of the polariton frequency for a monomolecular layer with $\hat{d} \| \hat{y}$. Wave vector $\vec{\kappa}$ is parallel to the x axis. There are two branches and the dotted lines show the width of the superradiant branch. Same parameters are used as in Fig. 2.

$$[\omega_y^2(\kappa) - \omega^2]\left[\left(\frac{c\kappa}{\omega}\right)^2 - \epsilon\right]^{1/2} = 3\pi \frac{\omega^3\gamma_0}{(\omega a/c)^2} . \qquad (3.50)$$

For real κ, these relations yield a two-branch spectrum somewhat similar to that found for $\hat{d} \| \hat{z}$ (see Fig. 7), the main difference being the damping of the superradiant branch for small values of κ. In Fig. 7 the radiative width of the radiative branch is shown by plotting $\mathrm{Re}\Omega(\kappa) \pm \mathrm{Im}\Omega(\kappa)$. The calculation is similar to the $\hat{d} \| \hat{z}$ case because on squaring Eq. (3.49) a polynomial of the third degree in ω^2 is obtained. As in the two previous polarizations the analytic properties $\gamma_\kappa = (\kappa^2 - k^2)^{1/2}$ cannot be reconciled with physical restrictions in the radiative region. However, we can, just as in the $\hat{d} \| \hat{z}$ cases, think of the decay of a prepared real-κ state as being exponential-like for small κ values with a width proportional to the imaginary part of $F_y(\omega, \kappa)$ evaluated at $\omega = \omega_y$. The label superradiant is appropriate because the right-hand side of Eq. (3.50) is approximately 10^4 times larger than the free-molecule damping width.

At $\kappa = 0$ the superradiant state is given by

$$\Omega^2(0) = \omega_y^2(0) - i(2\pi e^2 f_0/\epsilon a^2 m_e)k , \qquad (3.51)$$

which is identical in form with Eq. (3.42) because at $\kappa = 0$ there is no phase distinction between the wave vector and the direction of a $\vec{d}$ vector in the plane.

The y-polarized transitions also have a subradiant branch with dispersion similar to the z-polarized case. The radiation patterns have lobes with components in the direction of κ so that constructive interference is possible just as for z polarization.

A CAVM calculation along the lines of that outlined earlier in Sec. III B1 gives

$$[\omega'(\theta)]^2 = [\omega_y(0)]^2 - [\omega''(\theta)]^2 , \qquad (3.52)$$

where

$$\omega''(\theta) = \tfrac{1}{4}\omega_p^2 f_0 a(\cos\theta)^{-1} . \qquad (3.53)$$

Here, as in the z-polarized dipole case, the radiative width blows up near the light line. The turning point of the hairpin in Fig. 5 comes at an angle of 3.15° up from grazing. The radiative shift at this point is about 30 cm^{-1}. When the angle drops to 0.2° from grazing, the radiative shift is approximately 1.2×10^4 cm^{-1} or one-half of the exciton frequency. The end point occurs at an angle 0.16° up from grazing for $f_0 = 1.0$ and at 0.016° for $f_0 = 0.1$.

C. Scattering of light by a monolayer

We consider the scattering of a linearly polarized plane monochromatic wave of frequency ω by a monolayer in which the transition dipoles are polarized along $\hat{d} = \hat{x}$, $\hat{y}$, or $\hat{z}$. For a single excited state the equations of motion are

$$(\omega_0^2 - i\omega^3\gamma_0 - \omega^2)d_s = (e^2 f_0/m)[\hat{d} \cdot \vec{E}'(\vec{r}_s)]d_s , \qquad (3.54)$$

where $\vec{E}'(\vec{r}_s)$ is the exciting field at $\vec{r}_s$. The total electric field at an arbitrary field point not coincident with the lattice is

$$\vec{E}(\vec{r}) = \vec{E}_0(\vec{r}) + \sum_s \vec{\vec{F}}(\vec{r} - \vec{r}_s, \omega) \cdot \vec{d}_s , \qquad (3.55)$$

where $\vec{\vec{F}}$ is the retarded dipole-dipole dyadic. For an incident field

$$\vec{E}_0(\vec{r}) = \vec{E}_0 e^{i\vec{\kappa}\cdot\vec{r}} e^{ik_z z} \qquad (3.56)$$

and assuming the dipoles are modulated accordingly,

$$d_s = d e^{i\vec{\kappa}\cdot\vec{r}_s} , \qquad (3.57)$$

the following expression is obtained by using Eq. (3.54) to eliminate $\vec{d}_s$ from Eq. (3.55):

$$\vec{E}(\vec{r}) = \vec{E}_0 e^{i(\vec{\kappa}\cdot\vec{r} + k_z z)} + \frac{(e^2 f_0/m)(\hat{d} \cdot \vec{E}_0)}{\Omega_d^2(\kappa, \omega) - \omega^2} \sum_s \vec{\vec{F}}(\vec{r} - \vec{r}_s, \omega) \cdot \hat{d}\, e^{i\vec{\kappa}\cdot\vec{r}_s} , \qquad (3.58)$$

where $\Omega_d^2(\kappa, \omega)$ is defined in such a way that the three polariton dispersion equations (3.26), (3.41), and (3.49) can be written

$$\Omega_d^2(\kappa, \omega) - \omega^2 = 0 \qquad (3.59)$$

for $d = x$, y, and z.

We note that the second term on the right-hand side of Eq. (3.58), which is the amplitude for the

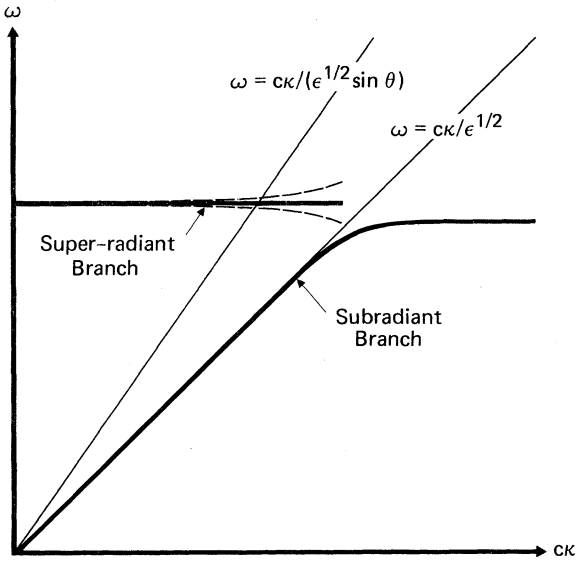

FIG. 8. Schematic diagram of the intersection of the light line of the host medium surrounding the monolayer with the superradiant branch.

scattered light, has a denominator that vanishes if Eq. (3.59) is satisfied for real ω and κ also satisfying

$$\epsilon(\omega/c)^2 = \kappa^2 + k_z^2 \ . \tag{3.60}$$

This occurs only for the trivial case $\hat{d} = \hat{z}$ and $\kappa = 0$, for which $\hat{d} \cdot \vec{E}_0 = 0$, so that there is no scattering.

In all other cases the denominator can become small but does not vanish because the dispersion curve for the incident photon [from Eq. (3.60)] cuts all the polariton curves on the left side of the light line in Figs. 2, 6, and 7, where all the states have finite widths. Thus the scattering amplitude has a resonance at the crossing point of Eq. (3.60) and a superradiant branch. This is shown schematically in Fig. 8, where θ is the angle of incidence so that $\kappa = \xi \sin\theta$, $k_z = \xi \cos\theta$, $\omega = c\xi\epsilon^{-1/2}$, and ξ is the magnitude of the incident-photon wave vector.

The scattering spectra have a particularly simple representation in terms of the real and imaginary parts of the CAVM frequencies. In Sec. III C1 we again separately consider the three dipole orientations treating only the reflection power spectra in detail.

1. *Scattering of p-polarized radiation*

a. Dipoles perpendicular to the plane ($\hat{d} \parallel \hat{z}$). The reflection power is defined as the z component of the Poynting vector S_z normalized to unit incident intensity. For p-polarized light

$$S_z \propto \mathrm{Re}(E_x H_y^*) \propto (\omega/ck_z)\left|E_x\right|^2 \ . \tag{3.61}$$

For this orientation the x component of the scattered field comes from taking the cross derivative of the Hertz vector (3.18). This leads to an expression for the reflection power,

$$R_z(\omega, \theta) = \frac{\omega^2 \gamma_{r,z}^2(\theta)\cos\theta}{\{[(\omega_z(0)]^2 - \omega^2\}^2 + \omega^2[\gamma_{t,z}(\theta)]^2} \ . \tag{3.62}$$

Here $\gamma_{r,z}(\theta)$ is twice the imaginary part of the CAVM frequency and

$$\gamma_{t,z}(\theta) = \gamma_{d,z}(\theta) + \gamma_{r,z}(\theta) \ , \tag{3.63}$$

where γ_d is the width on the nonradiative channels of decay. When $\theta = 0$ and $\frac{1}{2}\pi$ the reflection power is zero. In the former case the incident field is polarized perpendicular to the transition dipoles, which cannot then be driven by the incident field, while in the latter case the excited state has an infinite width so that the scattering amplitude for any one frequency is zero. For intermediate angles of incidence the band shape is Lorentzian with a peak at the exciton frequency $\omega_z(0)$ and a peak reflectivity of

$$R_z(\omega_z, \theta) = [\gamma_{r,z}(\theta)/\gamma_{t,z}(\theta)]^2 \cos\theta \ . \tag{3.64}$$

For larger θ the total decay rate $\gamma_{t,z}$ can become a significant fraction of ω_z, shifting the peak to the red, while broadening it asymmetrically. This can be seen more clearly by rearranging the denominator of Eq. (3.62):

$$R_z(\omega, \theta) = \frac{\omega^2[\gamma_{r,z}(\theta)]^2\cos\theta}{[\mathrm{Re}(\omega_{\mathrm{CAVM}}^2) - \omega^2]^2 + [\mathrm{Im}(\omega_{\mathrm{CAVM}}^2)]^2} \ , \tag{3.65}$$

where

$$\mathrm{Re}(\omega_{\mathrm{CAVM}}^2) = \omega_z^2 - 2[\omega''(\theta)]^2 = \omega_z^2 - \tfrac{1}{2}[\gamma_{t,z}(\theta)]^2 \tag{3.66}$$

and

$$\mathrm{Im}(\omega_{\mathrm{CAVM}}^2) = 2\omega'(\theta)\omega''(\theta) = \gamma_{t,z}\{\omega_z^2 - \tfrac{1}{4}[\gamma_{t,z}(\theta)]^2\}^{1/2} \ . \tag{3.67}$$

The frequency of the peak is given by the square root of Eq. (3.66). At the turning point in Fig. 5, the peak has shifted approximately 7 cm^{-1}, while $\gamma_{r,z}$ is approximately 1000 cm^{-1} at that point. The root of Eq. (3.66) is equivalent to the geometric mean $\omega_z \pm 2^{1/2}\omega''$, so that the bandwidth can get quite large while the peak shifts remain essentially undetectable.

b. Dipoles parallel to the wave vector $\vec{\kappa}$ ($\hat{d} \parallel \hat{z}$). Using Eq. (3.61) for S_z and Eqs. (3.36) and (3.37) for the electric field, the reflection power is found to be

$$R_x(\omega, \theta) = \frac{\omega^2[\gamma_{r,x}(\theta)]^2\cos^2\theta}{(\omega_x^2 - \omega^2)^2 + \omega^2[\gamma_{r,x}(\theta)]^2} \ . \tag{3.68}$$

The radiative width is always small so no dispersion in the peak frequency will be seen. The reflectivity is at a maximum at normal incidence and zero near grazing, where the lattice dipoles are perpendicular to the incident field.

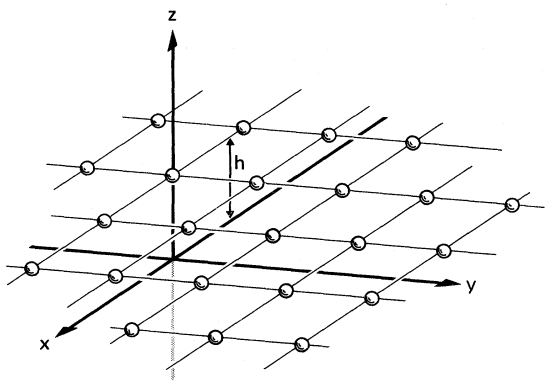

FIG. 9. Schematic representation of a monolayer of molecules at a height h above the plane interface between media with dielectric constants ϵ_1 ($z<0$) and ϵ_2 ($z>0$). Equation of the interface plane is $z=0$.

2. *Scattering of s-polarized radiation*

For s-polarized backscattering the Poynting vector is

$$S_z \propto -\mathrm{Re}(E_y H_x^*) \propto (ck_z/\omega)|E_y|^2 . \tag{3.69}$$

The expression for the reflection power is given by

$$R_y(\omega,\theta) = \frac{\omega^2\gamma_{r,y}^2\cos\theta}{(\omega_y^2-\omega^2)^2+\omega^2[\gamma_{r,y}(\theta)]^2} , \tag{3.70}$$

where the denominator can be rearranged in analogy to Eq. (3.65). Near $\theta=0$, the behavior of Eq. (3.70) is very similar to the x-polarized dipole case, while near grazing it behaves like the z-polarized case.

Intersection between the subradiant branch and an incident photon is not possible for a monolayer in a medium with dielectric constant ϵ. However, if the monolayer is adjacent to the interface of an optically denser medium; coupling to the evanescent field of the second medium may occur. This is the topic of Sec. IV.

IV. MONOLAYER NEAR A SUBSTRATE

To describe the optical properties of an ordered array of molecules located near the plane interface between optically distinct materials, a new coordinate system is introduced; see Fig. 9. The media are two half spaces with dielectric constants ϵ_2 ($z>0$) and ϵ_1 ($z<0$), and the plane $z=0$ separates the two. It is assumed that the monolayer sites are a distance h (>0) above the interface

$$\vec{r}_s = na\hat{x} + ma\hat{y} + h\hat{z} , \tag{4.1}$$

so that the monolayer lies entirely within the second medium. It is not essential to assume the lattice to be a square net.

The scattering of light by the monolayer may be treated by extensions of the method outlined in Sec. III C. For light incident from medium 2 the driving field consists of the incident field and a field due to reflection from the plane $z=0$. For light incident from medium 1 the driving field is the evanescent field if the angle of incidence $\theta>\theta_c$ (the critical angle), otherwise it is the propagating transmitted field.

The total field outside the monolayer has the same form as Eq. (3.58) for the medium containing the incident beam except that now the denominator of the scattered-wave part refers to polaritons of the coupled system monolayer and interface. The coupling arises through the interaction of the monolayer with image and surface fields. An essential first step in deriving a theory of light scattering by monolayers is, therefore, the derivation of the polariton dispersion equation by solving the equations of motion in the absence of a driving field.

We consider only the case of transitions polarized parallel to the z-axis. The Hertz vector for a single dipole at $\vec{r}_s$ at a height h above the interface can be obtained from the results of Baños,[18]

$$\frac{d_s}{\epsilon_2}\left(\frac{e^{ik_2|\vec{r}-\vec{r}_s|}}{|\vec{r}-\vec{r}_s|}+\frac{1}{2\pi}\int_{-\infty}^{\infty}\int d\xi\, d\eta\, \Gamma_2(\xi,\eta) \times e^{-\gamma_2(h+z)}\, e^{i[\xi(x-na)+\eta(y-ma)]}\right), \tag{4.2}$$

where

$$\Gamma_2(\xi,\eta) = (k_1^2\gamma_2 - k_2^2\gamma_1)(k_1^2\gamma_2 + k_2^2\gamma_1)^{-1} , \tag{4.3}$$

$$k_i^2 = \epsilon_i(\omega/c)^2, \quad i=1,2, \tag{4.4}$$

$$\gamma_i = (\xi^2+\eta^2-k_i^2)^{1/2} . \tag{4.5}$$

The Hertz vector for an array of dipoles d_s with modulation $e^{i\vec{k}\cdot\vec{r}_s}$ is obtained by summing Eq. (4.2) over sites s. After transforming the sum to one over reciprocal-lattice vectors $\vec{G}$ in a manner similar to that used in Sec. III B we obtain

$$\Pi_{2z}(\vec{r}) = \frac{2\pi d}{a^2\epsilon_2}\sum_{\vec{G}}\gamma_2^{-1}[e^{-\gamma_2|h-z|} + \Gamma_2(\vec{g})\, e^{-\gamma_2(h+z)}]e^{i\vec{g}\cdot\vec{\rho}} , \tag{4.6}$$

where

$$\vec{r} = (z,\vec{\rho}), \quad \vec{g} = \vec{k}+\vec{G}, \qquad \Gamma_2(g) = [k_1^2\gamma_2(\vec{g}) - k_2^2\gamma_1(\vec{g})][k_1^2\gamma_2(\vec{g}) + k_2^2\gamma_1(\vec{g})]^{-1} , \tag{4.7}$$

and

$$\gamma_i(\vec{g}) = (g^2-k_i^2)^{1/2} . \tag{4.8}$$

Henceforth the label $\vec{g}$ will be omitted from γ_i and Γ_2, where no confusion with Eqs. (4.3) and (4.5) is possible.

The first part of Eq. (4.6) is simply the Hertz vector of the monolayer in the absence of the substrate, so the second part is the entire contribution from image field and surface polarization fields.

The exciting field at $\vec{r}_s$ is obtained through the use of Eq. (3.21) and the limit $\vec{r} \to \vec{r}_s$ while subtracting out the self-field of the sth site. By analogy with Eq. (3.24) we write the result in the form

$$d^{-1}E'_{2z}(h) = -v_{2z}(\kappa, h) - i\tfrac{2}{3}k_2^3 + (2\pi\kappa^2/a^2\epsilon_2)\gamma_2^{-1}(1+\Gamma_2 e^{-2h\gamma_2}), \quad (4.9)$$

where both γ_2 and Γ_2 are evaluated for $\vec{G}=0$, and the short-range static dipole sum $v_{2z}(\kappa, h)$ includes a contribution from the image dipoles.

The polariton dispersion relation is

$$[\omega_{2z}^2(\kappa, h) - \omega^2](\kappa^2 - \epsilon_2\omega^2/c^2)^{1/2} = \frac{2\pi e^2 f_0}{m_e a^2 \epsilon_2}\kappa^2 \times[1+\Gamma_2(\kappa)e^{-2h(\kappa^2-\epsilon_2\omega^2/c^2)^{1/2}}], \quad (4.10)$$

where

$$\omega_{2z}^2(\kappa, h) = \omega_0^2 + \frac{e^2 f_0}{m_e} v_z(\kappa) - \frac{2\pi e^2 f_0}{m_e a^2 \epsilon_2}\sum_{\vec{G}}{}' g^2 \gamma_2^{-1}(\vec{g})\Gamma_2(\vec{g})\, e^{-2h\gamma_2(g)}. \quad (4.11)$$

In this last equation the second and third terms make up the total short-range interaction $v_{2z}(\kappa, h)$ in Eq. (4.9) and the prime signifies the omission of the $\vec{G}=0$ term.

The dispersion relation (4.10) is quite general in that the properties of medium 1 have not been specified except for the requirement that the magnetic permeability is unity. In particular Eq. (4.10) describes the coupling between polaritons of the monolayer and surface modes such as the surface-plasmon oscillations of a metal. This latter problem is of some interest in connection with the decay of coherent excitons at a metal surface. However, we shall not pursue the problem of exciton–surface-plasmon coupling any further in this paper.

Next let us consider the contribution from the substrate in ω_{2z}. For transparent insulating media we have $G \gg \kappa$ and $G \gg \epsilon_1^{1/2}\omega/c$ for all $\vec{G} \neq 0$ in the optical-frequency region, so that $\Gamma_2(g)$ simplifies to

$$\Gamma_2(g) = (\epsilon_1 - \epsilon_2)/(\epsilon_1 + \epsilon_2), \quad (4.12)$$

and the last term of Eq. (4.11) becomes, apart from the factor $e^2 f_0 (m_e\epsilon_2)^{-1}$,

$$-\frac{\epsilon_1 - \epsilon_2}{\epsilon_1 + \epsilon_2}\frac{2\pi}{a^2}\sum_{\vec{G}}{}' G e^{-2hG}. \quad (4.13)$$

Now the factor (4.12) is just that predicted by image theory in the electrostatic limit[23] and the sum is just the short-range part ($\vec{G}=0$ term omitted) of the interaction between a dipole at $\vec{r}=(h, 0)$ and a two-dimensional lattice of dipoles in the plane $z=-h$.[24] We therefore conclude that the substrate field only shifts the frequency of the mechanical exciton from $\omega_z(\kappa)$ to $\omega_{2z}(\kappa, h)$.

Finally we examine the additional damping introduced through the factor

$$F_2(\kappa) = 1 + \Gamma_2(\kappa)\, e^{-2h\gamma_2(\kappa)} \quad (4.14)$$

by the substrate. In the limit $\kappa \ll \omega/c$,

$$\Gamma_2(\kappa) = -(n_2 - n_1)/(n_2 + n_1), \quad (4.15)$$

where $n_i = \epsilon_i^{1/2}$ $(i=1, 2)$ is the refractive index and Eq. (4.15) is just the reflectivity for normal angles of incidence. Therefore,

$$F_2(\kappa) = 1 + R(\omega)\, e^{i2hn_2\omega/c} \quad (4.16)$$

oscillates periodically with the perpendicular separation of monolayer from the surface with no cutoff at large distances. This effect is quite different to that observed for a single molecule (or an incoherent exciton on a monolayer), for which the substrate contribution to the lifetime dies rapidly as h increases. If $n_1 \gg n_2$, the surface is highly reflecting, $R \simeq 1$, and for small h such that $2hn_2\omega/c \ll 1$ we have $F_2(\kappa) \simeq 2$. This is the image limit in which the transition dipoles and their electromagnetic images oscillate in phase, and the polariton dispersion curve differs from Fig. 2 mainly in the superradiant branch, which now has twice the width.

If $\kappa \gg \omega/c$, then $\Gamma_2(\kappa)$ is given by Eq. (4.12) and so

$$F_2(\kappa) = 1 + (\epsilon_1 - \epsilon_2)/(\epsilon_1 + \epsilon_2)\, e^{-2h\kappa}.$$

The substrate effect decays exponentially with distance.

In the intermediate region there is a range of frequencies such that $\kappa^2 > \epsilon_2\omega^2/c^2$ and $\kappa^2 < \epsilon_1\omega^2/c^2$. For this range γ_1 is pure imaginary and γ_2 is real. In this case radiative decay into the substrate is allowed, while emission into the host medium 2 is forbidden. This is typical of the attenuated-(ATR) and the frustrated-total-reflection (FTR) experiments where phase match of an evanescent wave of medium 1 to the nonradiant states of a second material is used to probe the properties of the latter. In Fig. 10 the crossing of the light line $\omega = c\kappa\epsilon_1^{-1/2}$ of medium 1 with the subradiant branch of the polariton is shown schematically. In principle the whole of the branch to the left of the point of intersection is mappable by using angles of incidence $\theta > \theta_c$ for medium 1.

V. DISCUSSION AND SUMMARY

The detection of superradiant and subradiant branches of the polariton spectrum has already been discussed at several places in this paper. Summarizing briefly we note that, in principle, the radiant branch can be detected by resonant light scattering either by a resonance fluorescence or a resonance Raman process with light incident from medium 2. The subradiant levels are observable in

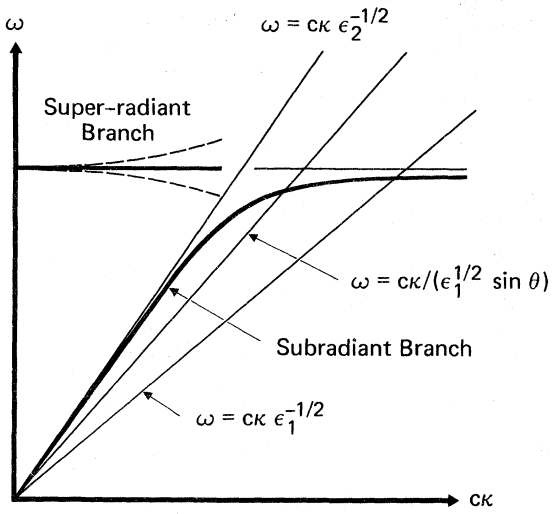

FIG. 10. Schematic diagram of the intersection of the light line of the substrate medium 1 with the subradiant branch of the polariton spectrum.

an internal-reflection experiment with light incident from medium 1 with an angle of incidence θ greater than the critical angle θ_c.[25]

The angular dependence of the radiative width of the CAVM for this system is identical in form to results derived for correspondingly polarized plasmon modes in thin metal foils[26,27] and phonon modes in thin ionic crystals.[22,28] In the former case, two surface-plasmon modes interact and become nondegenerate when the foil thickness decreases to less than the penetration depth of the surface mode. The lower-energy antisymmetric mode exhibits the same oscillating dipolar layer geometry as the z-polarized dipoles here. The coherent radiative decay of excitons in thin films considered by Lee *et al.*[11(b)] might also be profitably treated using constant-angle modes.

For monolayers of organic molecules the assembling technique developed so elegantly by Kuhn and his collaborators[1,29] has many advantages, the chief one being the ability to fix the distance of the absorbing monolayer at integral multiples of the arachidate chain length (20 Å) from the substrate. Unfortunately there is still not enough evidence concerning the crystallinity, i.e., the two-dimensional ordering, within the plane. However, effects of disorder can be minimized by using dyes with transitions perpendicular to the plane. One such dye, quinquithienyl,[1] has a very strong first singlet transition ($f_0 \simeq 1.0$) and monolayers containing a high concentration of this molecule might exhibit polariton effects of the type described in Secs. III and IV. Another good candidate is the dye transbixin methylester,[30] which forms monolayers with a distorted hexagonal-close-packing structure. A strong transition occurs at 2.6 eV in the free molecule polarized along the long axis and therefore perpendicular to the plane in the monolayer. Strong interactions occur on monolayer formation because the transition is observed to shift to 4.9 eV in the ultraviolet.

Finally we conclude with some comments on an entirely different type of monomolecular system, one which certainly has long-range order of the type invoked in the model. For the first singlet transition of some linear polyacene crystals like anthracene and tetracene, the exciton transfer interaction between the (001) planes is believed to be very weak in comparison with the in-plane interaction.[4-6] In these systems the gas-to-crystal shifts, arising from excited-state van der Waals interactions, are different for surface and bulk planes, and these shifts determine the relative order of the levels and whether the exciton is localized near the surface or delocalized in the bulk region. The surface plane can become decoupled from the rest of the crystal and one excited state corresponds to the exciton localized on this plane and nowhere else in the crystal.[4-6] Thus the surface plane reacts to an incident-light field like a monolayer sitting on a substrate of different physical properties. Surface systems of this type have polariton states that are modified in a more complicated way than when the substrate is transparent with a constant dielectric function, for ϵ_1 has ω-dependent real and imaginary parts. The theory presented in this paper is a first step in trying to understand the physics of these unusual systems.

ACKNOWLEDGMENT

We wish to thank H. Morawitz for discussions that helped us to sharpen our ideas on certain aspects of this work.

[1](a) H. Kuhn, D. Möbius, and H. Bucher, in *Physical Methods of Chemistry*, edited by A. Weissberger and B. W. Rossiter (Wiley-Interscience, New York, 1972), Pt. III B, Chap. VII. (b) K. H. Drexhage, Prog. Opt. 12, 165 (1974).

[2]J. L. Gland and G. A. Somorjai, Surf. Sci. 38, 157 (1973).

[3]D. Chapman, *Biological Membranes* (Academic, New York, 1968).

[4]M. S. Brodin, M. A. Dudinskii, and S. V. Morisova, Opt. Spectrosc. 31, 401 (1971); 34, 1120 (1973).

[5]J-M. Turlet and M. R. Philpott, J. Chem. Phys. 62, 2777 (1975).

[6]J.-M. Turlet and M. R. Philpott, J. Chem. Phys. 62, 4260 (1975).

[7]D. V. Sivukhin, Zh. Eksp. Teor. Fiz. 18, 976 (1948); 21, 367 (1951); 30, 374 (1956) [Sov. Phys.-JETP 3, 269 (1956)].

[8]C. Strachan, Proc. Camb. Philos. Soc. 29, 116 (1932).
[9]G. A. Bootsma and F. Meyer, Surf. Sci. 14, 52 (1969).
[10]P. W. Atkins and A. D. Wilson, Surf. Sci. 22, 433 (1970).
[11](a) V. M. Agranovich and O. A. Dubovskii, Zh. Eksp. Teor. Fiz. Pis'ma Red. 3, 345 (1966) [JETP Lett. 3, 223 (1966)]; (b) Y. C. Lee and P. S. Lee, Phys. Rev. B 10, 344 (1974); K. C. Liu, Y. C. Lee, and Y. Shan, Phys. Rev. B 11, 978 (1975).
[12]M. R. Philpott, J. Chem. Phys. 61, 5306 (1974).
[13]See, for example, M. R. Philpott, Adv. Chem. Phys. 23, 227 (1973).
[14]F. W. DeWette and G. E. Schacher, Phys. Rev. 137, A78 (1965).
[15]H. Benson and D. L. Mills, Phys. Rev. 178, 839 (1969).
[16]J. R. Ackerhalt, P. L. Knight, and J. H. Eberley, Phys. Rev. Lett. 30, 456 (1973).
[17]J. E. Sipe and J. Van Kranendonk, Phys. Rev. A 9, 1806 (1974).
[18]A. Baños, Jr., *Dipole Radiation in the Presence of a Conducting Half-Space* (Pergamon, London, 1966).
[19]The electric field of a lattice of static dipoles is obtained by setting $k=0$ in Eq. (3.22). The short-range part of this field is defined to be the sum of all $\vec{G}\neq 0$ Fourier terms. The long-range part, which is the $\vec{G}=0$ term, is not singular in the limit $\vec{r}\to\vec{r}_s=0$, and gives the long-range dipole sum mentioned in Sec. III A. For excitations in the optical range of frequencies, $\vec{G}\gg k$ for all $\vec{G}\neq 0$, so that the sum of all non-null G terms in the retarded field (3.22) essentially equals the short-range field of static dipoles. After subtraction of the self-field at site $\vec{r}_s=0$ this short-range field contributes $v_s(\kappa)$ in Eq. (3.24) for the exciting field.
[20]V. M. Agranovich and V. L. Ginzburg, *Spatial Dispersion in Crystal Optics and the Theory of Excitons* (Wiley-Interscience, New York, 1966).
[21]M. Born and E. Wolf, *Principles of Optics*, 4th ed. (Pergamon, London, 1970), p. 81.
[22]K. L. Kleiwer and R. Fuchs, Phys. Rev. 150, 573 (1966).
[23]The electrostatic image of a charge e in medium 2 is a charge $e'=-[(\epsilon_2-\epsilon_1)/(\epsilon_2+\epsilon_1)]e$ in medium 1. For an ideal conductor we have $|\epsilon_1|\gg|\epsilon_2|$ and $e'=-e$.
[24]See, for example, Eq. (14) in M. R. Philpott, J. Chem. Phys. 58, 588 (1973).
[25]C. K. Carniglia, L. Mandel, and K. H. Drexhage, J. Opt. Soc. Am. 62, 479 (1972).
[26]K. L. Kleiwer and R. Fuchs, Phys. Rev. 153, 498 (1967).
[27]W. Steinman, Phys. Status Solidi 28, 437 (1968).
[28]D. W. Berreman, Phys. Rev. 30, 2193 (1963). Note especially Eqs. (3) and (4).
[29]K. H. Drexhage, *Optische Untersuchungen an neuartigen monomolekularen Farbstoffschichten* (Habilitations-Schrift, University of Marburg, Germany, 1966).
[30]J. A. Bergeron and G. M. Slusarczuk, unpublished results, quoted by G. D. Mahan, in *Proceedings of the Advanced Study Institute on Electronic Structure of Polymers and Molecular Crystals*, edited by J. André, J. Ladik, and J. Delhalle (Plenum, New York, 1975).